

Lawrence Berkeley National Laboratory

LBL Publications

Title

Low temperature acclimation with electrical stimulation enhance the biocathode functioning stability for antibiotics detoxification

Permalink

<https://escholarship.org/uc/item/3rz453d3>

Journal

Water Research, 100

ISSN

0043-1354

Authors

Liang, Bin

Kong, Deyong

Ma, Jincai

et al.

Publication Date

2016-09-01

DOI

10.1016/j.watres.2016.05.028

Peer reviewed

Low temperature acclimation with electrical stimulation enhance the biocathode functioning stability for antibiotics detoxification

Author links open overlay panel [BinLiang^{abc}](#) [DeyongKong^{ab}](#) [JincaiMa^c](#) [ChongqingWen^c](#) [TongYuan^c](#) [Duu-JongLee^{bf}](#) [JizhongZhou^c](#) [AijieWang^{ab}](#)

Show more

<https://doi.org/10.1016/j.watres.2016.05.028> Get rights and content

Highlights

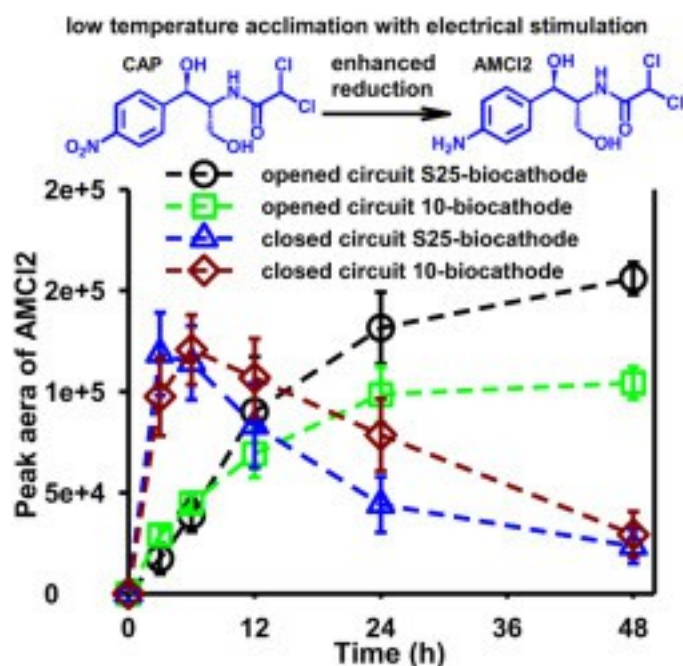
- Low temperature acclimation with electrical stimulation enhanced biocathode stability.
 - 10-biocathode obviously enhanced the chloramphenicol nitro group reduction efficiency.
 - Temperature elevation significantly altered the 10-biocathode communities structure.
 - 10 °C acclimated biocathode (10-biocathode) maintained electron transfer related genes.
 - 10-biocathode selectively enriched cold-adapted nitroaromatics reducers.

Abstract

Improvement of the stability of functional [microbial communities](#) in [wastewater](#) treatment system is critical to accelerate pollutants [detoxification](#) in cold regions. Although biocathode communities could accelerate environmental [pollutants degradation](#), how to acclimate the cold stress and to improve the catalytic stability of functional microbial communities are remain poorly understood. Here we investigated the [structural and functional responses](#) of [antibiotic](#) chloramphenicol (CAP) reducing biocathode communities to constant low temperature 10 °C (10-biocathode) and temperature elevation from 10 °C to 25 °C (S25-biocathode). Our results indicated that the low temperature [acclimation](#) with electrical stimulation obviously enhanced the CAP nitro

group [reduction](#) efficiency when comparing the [aromatic amine](#) product AMCl₂ formation efficiency with the 10-biocathode and S25-biocathode under the opened and closed circuit conditions. The 10-biocathode generated comparative AMCl₂ maximum as the S25-biocathode but showed significant lower dehalogenation rate of AMCl₂ to AMCl. The continuous low temperature and temperature elevation both enriched core functional community in the 10-biocathode and S25-biocathode, respectively. The 10-biocathode functioning stability maintained mainly through selectively enriching cold-adapted functional species, coexisting metabolically similar nitroaromatics reducers and maintaining the [relative abundance](#) of key [electrons transfer](#) genes. This study provides new insights into biocathode functioning stability for accelerating environmental pollutants degradation in cold wastewater system.

Graphical abstract



1. [Download high-res image \(255KB\)](#)

2. [Download full-size image](#)

- [Previous](#) article in issue
- [Next](#) article in issue

Keywords

Antibiotics degradation

Low temperature

Electrical stimulation

Biocathode communities

Functioning stability

1. Introduction

Low temperature could strongly reduce the rates of [microbial growth](#) and biochemical reactions ([D'Amico et al., 2006](#)). Most reactions involved in organic matter [biodegradation](#) require more energy to proceed at low temperatures than at mesophilic conditions ([Lettinga et al., 2001](#)). [Environmental temperature](#) perturbations universally appear in cold regions. The development of cold-adapted biocatalysis system would be of great economical importance because it could avoid a heavy economy burden on [wastewater](#) heating process ([Lettinga et al., 2001](#), [McKeown et al., 2012](#)). Therefore, how to acclimate the cold stress and to improve the catalytic stability of functional [microbial communities](#) in [wastewater treatment](#) system is critical to accelerate environmental pollutants biotransformation/detoxification under lower temperature conditions.

At the global scale, the widespread abuse of [antibiotics](#) has led to their release into various environmental settings. As a result, residues of those antibiotics are frequently detected in diverse water environments including [sewage treatment](#) plant influent/effluent, livestock wastewater [effluent](#), hospital effluent, and urban rivers ([Kong et al., 2015a](#), [Zhang et al., 2015a](#)). Their persistence in the environment could potentially evolve antibiotic-resistant bacteria and even multi-drug resistant bacteria, which constitute a great risk for human health ([Andersson and Hughes, 2014](#)). Thus, antibiotics in wastewater must be degraded to eliminate their antibacterial activity before discharging into the environment.

Bioelectrochemical system (BES) has been developed for the cathodic [reduction](#) of various organic pollutants including nitroaromatics, azo dyes, halogenated aromatics, [alkanes](#) and [ethylenes](#) ([Feng et al., 2015](#), [Liang et al., 2014](#), [Mu et al., 2009](#), [Radjenovic et al., 2012](#), [Shen et al., 2013](#), [Strycharz et al., 2008](#), [Strycharz et al., 2010](#), [Wang et al., 2011](#)). Recently, antibiotics such as chloramphenicol (CAP), florfenicol, metronidazole, nitrofurazone and furazolidone, which are widely used in China, could be effectively reduced to antibacterial inactivity products with abiotic [cathode](#) or biocathode ([Kong et al., 2015a](#), [Kong et al., 2015b](#), [Liang et al., 2013](#)). Moreover, biocathode displayed higher pollutants reduction efficiency and selectivity, lower reduction overpotentials than those of the abiotic cathodes ([Liang et al., 2013](#), [Liang et al., 2014](#), [Wang et al., 2011](#)). The electrical stimulation could also simultaneously improve the [salinity](#) resistance and halogenated nitroaromatics removal

efficiency in biocathode communities ([Feng et al., 2015](#)). Additionally, a previous study revealed that the [catalytic activity](#) of ambient temperature acclimatized CAP-degrading biocathode was obviously decreased when the temperature dropped from 25 °C to a low temperature 10 °C ([Kong et al., 2014](#)). Although biocathode showed some promising advantages, little is known about whether low temperature [acclimation](#) with electrical stimulation could enhance the biocathode functioning stability for antibiotics [detoxification](#), especially from [phylogenetic](#) and functional genes perspectives.

In this study, we investigated the kinetics of antibiotic CAP degradation and main antibacterial inactivity products formation by biocathode communities under constant low temperature 10 °C and switching from 10 °C to 25 °C under opened and closed circuit conditions. Both the phylogenetic and functional communities within CAP-degrading biocathode were characterized using a comprehensive microarray GeoChip (v4.6) and 16S rRNA gene based Illumina MiSeq [sequencing](#) technologies. Important functional genes involved in [electron transfer](#) and nitroaromatics reduction in the two temperatures performed biocathode communities were also analyzed. The objectives of the current study were to (i) investigate how the low temperature acclimation and temperature elevation impacts phylogenetic and functional structure and composition of CAP-degrading biocathode communities, and (ii) reveal the improvement mechanisms of the low temperature acclimation with electrical stimulation on the biocathode functioning stability. Our results provide a new strategy to enhance the functioning stability of biocathode communities for accelerating environmental pollutants treatment in cold wastewater system.

2. Materials and methods

2.1. Microbial inoculum and BES tests

The BES reactors were constructed by assembling two equal-sized Lexan plates ($4 \times 4 \times 3 \text{ cm}^3$) with a cylindrical cavity (3 cm in diameter and 4 cm in length) and two equal-sized Lexan plates ($4 \times 4 \times 1 \text{ cm}^3$) as outside baffles and separated by a cation exchange membrane (Ultrex CMI-7000, Membranes International, Ringwood, NJ, U.S.) as described elsewhere ([Kong et al., 2015a](#)). The internal volumes of [anode](#) and [cathode](#) chambers were 28 mL each. [Graphite](#) fiber brush (2.5 cm in diameter and 2.5 cm in length, TOHO TENAX Co., Ltd., Japan) was used as anode and cathode. A 10 Ω resistor with the external power (0.5 V) in series was employed for the connection. A saturated calomel reference [electrode](#)(SCE, 0.247 V vs standard hydrogen electrode, SHE) (model-217, Shanghai Precise. Sci. Instrument Co., Ltd.,

China) was inserted into the cathode chamber. All of the potential data showed herein were against SHE. When the external power source and the resistor were disconnected, the BES was operated as the opened circuit biocathode mode. The experiment with the opened circuit biocathode lasted for 48 h, hence should have negligible effects on the [biofilm](#) communities.

Twelve biocathode BES reactors were started up at low temperature (10 °C) with 0.5 V [voltage](#) supply. Bioanode and biocathode in the BES were enriched by inoculating municipal [sludge](#) from a [wastewater treatment plant](#) (Harbin, China) and pre-enriched CAP-reducing consortium respectively as described elsewhere ([Liang et al., 2013](#), [Wang et al., 2011](#)). Afterwards, the 12 biocathode BESs were operated for 6 fed-batch cycles at 10 °C. Then 6 biocathode BESs of them were continued to run at 10 °C for another 6 cycles (the corresponding biofilms were labeled as 10-biocathode), and the other 6 biocathode BESs were switched from 10 °C to 25 °C and were run 6 cycles (the corresponding biofilms were termed as S25-biocathode). The actual cathode potentials fluctuated approximately <2% and 3% between the two biocathode groups before and after the temperature switchover, respectively. This small variation in the cathode potential should have minimal effects on the overall efficiencies of bioelectrochemical CAP [reduction](#) and products formation. The temperature (10 °C or 25 °C) throughout the experiment was maintained in a constant temperature incubator (BI-250A, STIK, Shanghai, China). In the biocathode mode, CAP (30 mg/L), [glucose](#) (600 mg/L) and cathode were the cathodic electron acceptor, intracellular and extracellular electron donors for cathodophilic microbes, respectively. At the end of the tests, the 12 cathode biofilms were sampled and stored at -20 °C until [DNA](#) extraction.

2.2. 16S rRNA gene sequencing, GeoChip hybridization and data analysis

A detailed description of the DNA extraction, DNA purity and quantity determination, PCR amplification, 16S rRNA gene Illumina MiSeq [sequencing](#), GeoChip [hybridization](#) and data analysis is provided in the [Supporting Information \(SI\)](#). Six 10-biocathode and S25-biocathode biofilms respectively were selected for the 16S rRNA gene Illumina MiSeq sequencing analysis. A total 10 cathode biofilms were selected for the GeoChip hybridization analysis. Extracted DNA (1.0 µg) from each sample was labeled with Cy-3 dye and then hybridized with GeoChip v4.6 as described previously ([Tu et al., 2014](#)). The spots with [signal-to-noise ratios](#) (SNR) lower than 2 were removed before statistical analysis ([He et al., 2010](#)).

The raw data from 16S rRNA gene sequencing was analyzed according to a recent study ([Qu et al., 2015](#)). Microbial [diversity indices](#) including Chao1 value, richness (identified OTU or detected functional gene numbers in each sample), Shannon-Weaver index (H) and Simpson reciprocal ($1/D$) were calculated as described elsewhere ([Schloss et al., 2009](#)). Detrended [correspondence analysis](#) (DCA), three nonparametric tests (multiple-response permutation procedure [MRPP], permutational [multivariate analysis](#) of variance [Adonis], and analysis of similarity [ANOSIM]) were calculated using R v2.15.1. Hierarchical clustering analysis was performed using CLUSTER v3.0 and visualized by TREEVIEW. All detected functional genes and identified OTUs at least 2 out of 5 or 6 biological replicates were used for the statistical analysis. Differences between treatments were statistically analyzed by the two-tailed unpaired t -test.

2.3. Chemicals and analytical methods

CAP (>98% purity) and high performance [liquid chromatography](#) (HPLC) grade [methanol](#) were purchased from Sigma-Aldrich (St. Louis, MO, U.S.). Other chemicals used in this study were of analytical grade.

[Effluent](#) samples taken from the cathode chamber within 48 h were filtered through a 0.22 μm filter (Shanghai XingYa Purification Material Co., China) before chemical analysis. The concentrations of CAP, the CAP transformation products CAP-NO (nitroso intermediate of CAP), AMCl_2 (the nitro-group reduced product of CAP, namely [aromatic amine](#) AMCl_2), AMCl (the partially dechlorinated product of AMCl_2), CAP-acetyl (acetylation of 3-hydroxyl of CAP to form CAP-acetyl) were measured using a reverse-phase HPLC system ([Liang et al., 2013](#)). The CAP transformation products were identified by a HPLC-MS as described recently ([Kong et al., 2015a](#), [Liang et al., 2013](#)). The rate constants of CAP reduction (k_{CAP}) and terminal product AMCl formation (k_{AMCl}) were calculated by fitting the data to apparent first-order reaction models: $C = C_0 e^{-kt}$ and $C = C_0 (1 - e^{-kt})$, respectively, where C represents the CAP (mg/L) or AMCl concentrations at time t (h), C_0 is the initial CAP concentration (30 mg/L) or maximal AMCl yield ($Y_{\text{max-AMCl}}$). The [electric current](#) (I) was calculated by the Ohm's law. CAP reduction efficiency ($E_{\text{r-CAP}}$, %) was evaluated based on the difference between influent and effluent CAP concentrations.

To characterize the bioelectrochemical activity of biocathode communities under different temperatures, cyclic voltammetry (CV) analysis was performed using an electrochemical workstation (model-660D, CH Instruments Inc., Austin, TX, U.S.) as described previously ([Liang et al., 2013](#)). To characterize the [microbial growth](#) activity of biocathode under different temperatures, the 10-biocathode and S25-biocathode

biofilms were stained with the LIVE/DEAD BacLight Bacterial Viability Kit (L7012, Molecular Probes, Invitrogen, Carlsbad, CA, U.S.) according to the manufacturer's instructions and then visualized under a confocal [laser scanning microscopy](#) (CLSM, ZEISS LSM 700, German). The bacterial staining kit was developed based on the bacterial membrane permeability and is commonly used to distinguish bacteria with high (green) or low (red) growth activity rather than determine whether the cells are living or dead ([Yang et al., 2015](#)).

3. Results and discussion

3.1. Functioning stability of the 10-biocathode subjected to temperature switchover

The CAP [reduction](#) and the terminal product AMCI formation efficiencies and rate constants in the 25 °C and 10 °C enriched biocathodes under decrease or elevation of 15 °C disturbances were compared. Our previous study indicated that the E_{r-CAP} (e.g. at 3 and 12 h), k_{CAP} , $Y_{max-AMCI}$ (at 24 h), and k_{AMCI} were all markedly decreased ($P < 0.001$) when decreasing the temperature from 25 to 10 °C ([Table 1](#)) ([Kong et al., 2014](#)). In the current study, the catalytic functioning stability of the 10-biocathode communities and the response of those communities to the temperature elevation were studied. The results indicated that the E_{r-CAP} (e.g. at 3 and 12 h) and k_{CAP} were not significantly differed when elevating temperature from 10 to 25 °C. Though the S25-biocathode had obviously higher k_{AMCI} (0.15 vs 0.10 h⁻¹; $P = 0.002$), $k_{AMCI2-AMCI}$ (calculating between 6 and 48 h; 0.046 vs 0.028 h⁻¹) and early AMCI yield (at 3 h, $P = 0.017$) than those of the 10-biocathode, the $Y_{max-AMCI}$ (at 48 h) was not significantly differed between the two operational groups ([Table 1](#)).

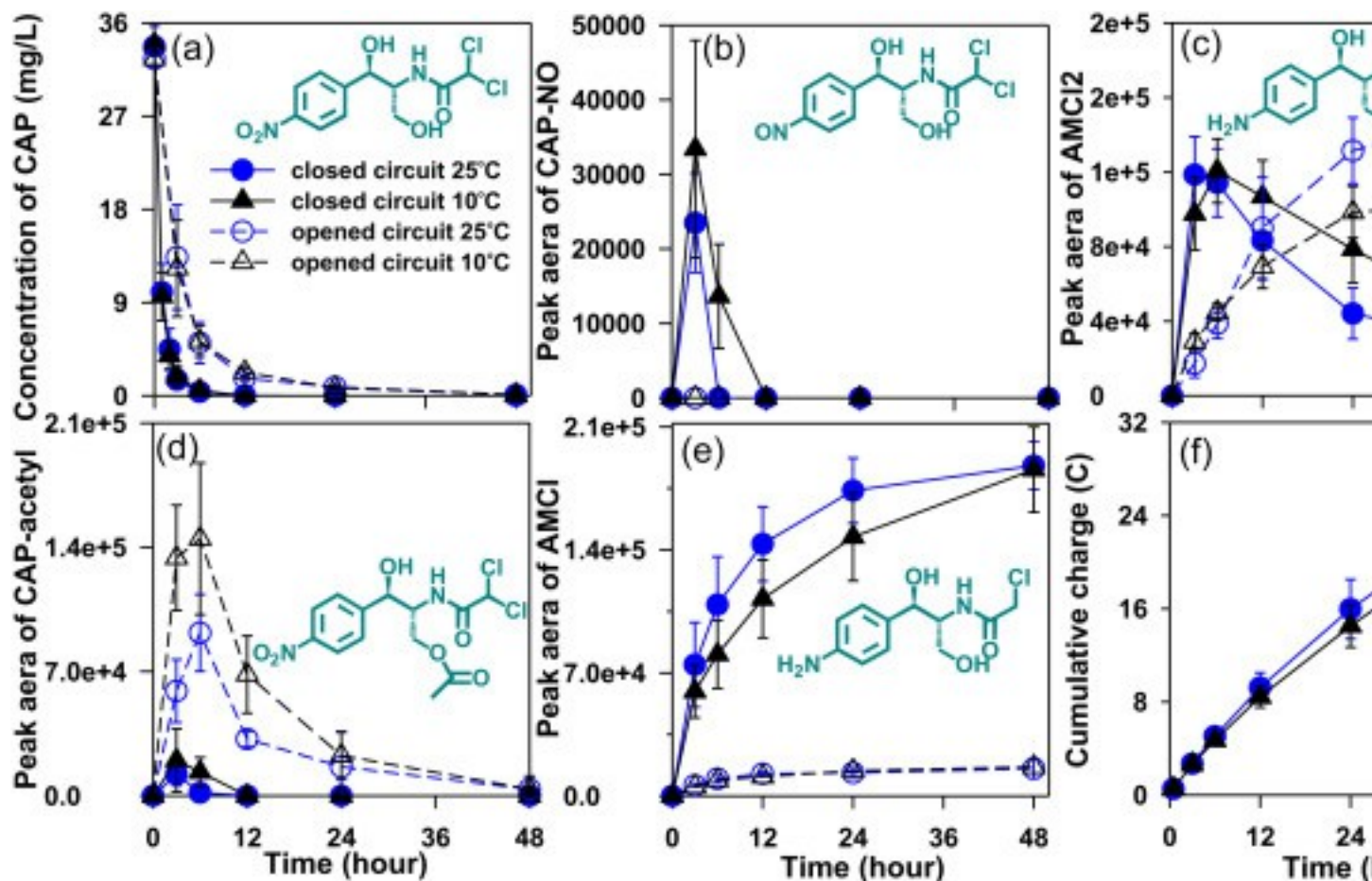
Table 1. Assessing the functioning stability of biocathode communities upon [environmental temperature](#) disturbances with the CAP [reduction](#) and terminal product AMCI formation efficiencies as indicators.

	25 °C	25 °C → 10 °C	P value	10 °C	10 °C → 25 °C	P value
CAP- $E_{r3h}/\%$	94.54 ± 2.79	86.60 ± 4.67	<0.001	94.69 ± 2.73	95.45 ± 2.51	0.366
CAP- $E_{r12h}/\%$	99.55 ± 0.51	97.70 ± 1.07	<0.001	100 ± 0.00	99.95 ± 0.24	0.330
CAP- k (h ⁻¹)	0.88 ± 0.08	0.63 ± 0.07	<0.001	1.22 ± 0.25	1.15 ± 0.18	0.630
AMCI- Y_{3h}	39,377 ± 13318	11,260 ± 3630	<0.001	59,540 ± 15,009	74,683 ± 24,096	0.017
AMCI- Y_{max}	81,670 ± 6167	51,153 ± 4837	<0.001	185,633 ± 24,305	187,868 ± 13,562	0.661
AMCI- k (h ⁻¹)	0.20 ± 0.05	0.06 ± 0.01	<0.001	0.10 ± 0.02	0.15 ± 0.02	0.002

Bold represents the P value <0.05.

3.2. Electrical stimulation increases the functioning stability of 10-biocathode

In order to demonstrate the functioning stability was increased in the 10-biocathode by the electrical stimulation with low temperature [acclimation](#), CAP reduction and the products (CAP-NO, AMCl₂, AMCl and CAP-acetyl) formation efficiencies were compared between the opened and closed circuit biocathodes under two operational temperatures, respectively. The results showed that the electrical stimulation significantly enhanced the biocathodic reduction of CAP to AMCl₂, and the reductive [dechlorination](#) of AMCl₂ to AMCl ([Fig. 1a, c, e](#)), which was consistent with our previous study ([Liang et al., 2013](#)). The k_{CAP} of the opened circuit S25-biocathode ($0.295 \pm 0.083 \text{ h}^{-1}$) was close to the opened circuit 10-biocathode ($0.326 \pm 0.074 \text{ h}^{-1}$) ($P = 0.60$). While the accumulation of the AMCl₂ yield (at 48 h) obviously increased in the opened circuit S25-biocathode compared to that of the opened circuit 10-biocathode ($P < 0.0001$). The opened circuit biocathode did not accumulate CAP-NO product ([Fig. 1b](#)). Thus, the increased AMCl₂ accumulation in the opened circuit S25-biocathode could be attributed to the fact that the opened circuit 10-biocathode generated more CAP-acetyl product (acetylation of 3-hydroxyl of CAP to form CAP-acetyl by bacterial CAP acetyltransferase) ([Shaw and Leslie, 1991](#)) especially between 3 and 12 h than those of the opened circuit S25-biocathode ($P < 0.09$). The bioelectrochemical reduction process could weaken the non-redox CAP acetylation reaction ([Fig. 1d](#)). The AMCl₂ yield (at 48 h) was not significantly differed between the closed circuit 10-biocathode and S25-biocathode ($P = 0.11$) ([Fig. 1c](#)). Between 12 and 24 h, the closed circuit 10-biocathode showed obviously lower AMCl yield and higher AMCl₂ yield ($P < 0.0006$). Nearly the same $Y_{\text{max-AMCl}}$ was generated regardless of opened ($P = 0.84$) and closed ($P = 0.66$) circuit conditions between the two biocathode groups, indicating the anaerobic dehalogenation of AMCl₂ to AMCl was temperature insensitive.



1. [Download high-res image \(695KB\)](#)
2. [Download full-size image](#)

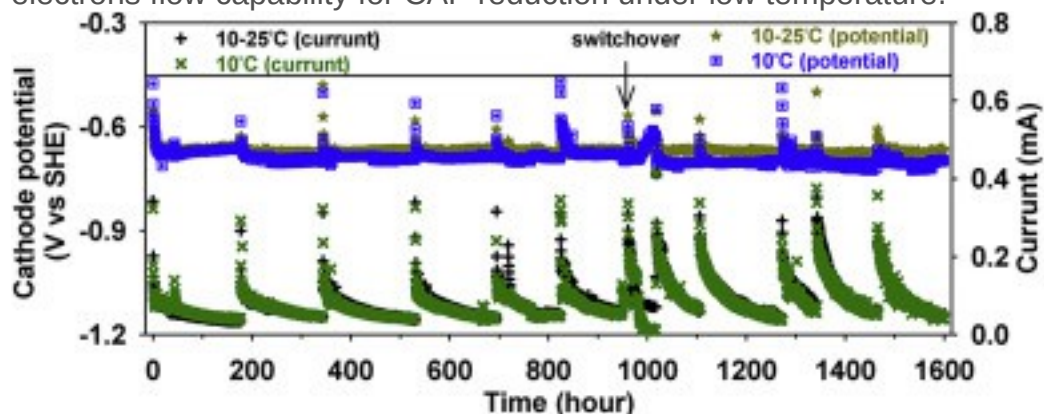
Fig. 1. Comparison of the CAP degradation (a), the products CAP-NO (b), AMCl₂ (c), CAP-acetyl (d) and AMCl (e) formation efficiencies between the opened and closed circuit biocathodes, as well as the cumulative charge during CAP degradation with the closed circuit biocathode (f) under constant 10 °C and switched 25 °C.

Additionally, in order to exclude the differences derived from the pure electrochemical reduction process between 10 and 25 °C, the CAP reduction and products generation efficiencies were assessed. The results showed that the k_{CAP} and AMCl₂ generation dynamics were not significantly differed between the two temperature abiotic [cathode](#) groups. The AMCl and CAP-NO yields showed no obvious differences at tested time points excepting the yields of AMCl at 48 h and NO at 24 h were significantly higher ($P = 0.069$) and lower ($P = 0.044$) under 10 °C, respectively ([Fig. S1](#)). Moreover, the 10-biocathode and S25-biocathode group (actually performed at 10 °C) showed no significant differences for the k_{CAP} , k_{AMCl} and $Y_{\text{max-AMCl}}$ ($P > 0.10$) before the temperature elevation. Collectively, these results indicated that the low temperature acclimation with

electrical stimulation enhanced the functioning stability of 10-biocathode for the CAP reduction especially for the reduction of the CAP nitro group to form AMCl_2 when comparing the AMCl_2 formation efficiencies of the 10-biocathode and S25-biocathode under the opened and closed circuit conditions, and the 10°C-acclimated biocathode showed more adaptive ability to [environmental temperature](#) changes than the 25°C-acclimated biocathode. These results highlight that the 10-biocathode BES could serve as a potential biotechnology unit for [wastewater](#) treatment in cold regions.

3.3. The bioelectrochemical feature of biocathode communities

The biocathode potential and the reaction current during the bioelectrochemical CAP reduction were monitored under 10 °C and 25 °C, respectively. The potential and current were at nearly the same level between the two biocathode groups under 10 °C. The current decreased to 0.1 mA level when the cathode electron acceptor CAP was depleted. After the temperature elevation, the potential and current were similar ([Fig. 2](#)) and the cumulative charge during CAP reduction between the S25-biocathode and 10-biocathode was not significantly different ([Fig. 1f](#)), both of which suggests that cathodophilic microbes under 10 °C could capture comparable electrons from cathode compared to those under 25 °C. Moreover, the biocathode communities showed the functioning stability to the temperature elevation as well as the cold-adapted and steady electrons flow capability for CAP reduction under low temperature.



1. [Download high-res image \(225KB\)](#)
2. [Download full-size image](#)

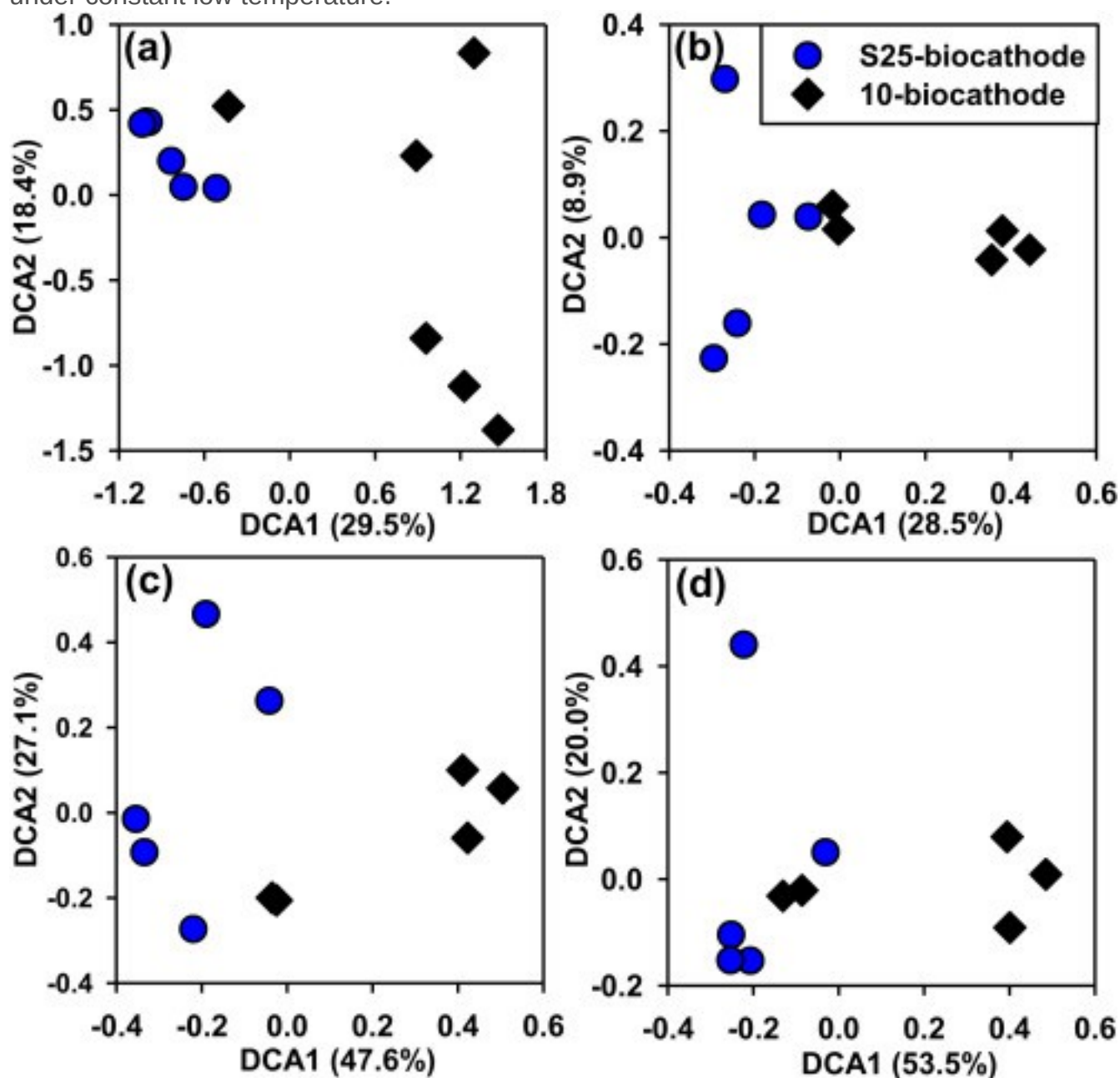
Fig. 2. The [cathode](#) potential and current of the CAP-reducing biocathodes performed under 10 °C and 10–25 °C (switchover from 10 °C to 25 °C). The arrow indicates that the 6 10-biocathodes were switched to the 25 °C cultivation (in short 10–25 °C group). Before the temperature switchover, all the 12 biocathodes operated at 10 °C.

The growth activity of 10-biocathode and S25-biocathode cells were analyzed with SYTO 9 (green indicates high growth activity of cells) and propidium [iodide](#) staining (red notes low growth activity of cells). The CLSM micrographs showed that biocathode communities had comparative total cathodophilic cells before and after the temperature elevation. The 10-biocathode showed relatively lower low-growth activity cells than that of the S25-biocathode by preliminarily observing from CLSM ([Fig. S2](#)), which demonstrated that the success of the low temperature acclimation of filtrated cold-adapted cathodophilic microbes. Additionally, the sudden elevation of 15 °C might affect the growth activity of the dominant cold-adapted microbes within biocathode communities. In order to determine no obvious differences in electrochemically [catalytic activity](#) between the two biocathodes, the CV analysis was employed. The result indicated that the CV characterization of the 10-biocathode and S25-biocathode were nearly consistent, such as the reaction current and reduction potential of nitro group (nitro group reduction was started at around -0.25 V). Further negative scanning on cathode potential (>-0.6 V), much higher cathode current was generated in both biocathodes. The hydrogen evolution reaction of the 10-biocathode and S25-biocathode were also similar ([Fig. S2](#)). These results showed that the low temperature acclimation and temperature elevation did not affect the electrochemically catalytic activity of biocathode communities, which was consistent with no obvious differences of the E_{r-CAP} , $Y_{max-AMCl}$ and cumulative charge between the two biocathode groups.

3.4. Shift of overall biocathode communities structure

To identify whether the low temperature acclimation enriches core functional species and the temperature elevation affects the [phylogenetic](#) (16S rRNA gene and *gyrB*) and functional structure and composition of CAP-reducing biocathode communities, hierarchical clustering analysis ([Fig. S3](#)) and detrended [correspondence analysis](#) (DCA) ([Fig. 3](#)) were carried out with the identified OTUs (in total 1798) and detected functional genes (in total 48,434). The results showed that the 10-biocathode were well separated from the S25-biocathode from phylogenetic and functional genes perspectives. Interestingly, the 10-biocathode and S25-biocathode communities could not be well separated at the [electrons transfer](#) related genes (in total 394) level ([Fig. 3](#)). The results of three nonparametric multivariate statistical approaches (ANOSIM, Adonis and MRPP) also strongly indicated that the 10-biocathode communities structure were obviously differed from the S25-biocathode communities. All the functional genes, 16S rRNA gene, *gyrB* and functional gene categories in biocathode communities were significantly differed between the two biocathode groups. Compared with other functional gene

categories ($P \leq 0.05$), the electrons transfer related genes and specific [cytochrome c](#) genes showed a relatively higher similarity ($P < 0.065$) between the two biocathode groups ([Table S1](#)). Taken the relationship between biocathode catalytic function and important electron transfer efficiency and characterization into account, the 10-biocathode and S25-biocathode had comparative bioelectrochemical features during CAP reduction. Therefore, the relatively unobvious difference in electron transfer related genes structure likely attributed to maintaining the electrons transfer efficiency and functioning stability of the bioelectrochemical CAP reduction under constant low temperature.



1. [Download high-res image \(393KB\)](#)
2. [Download full-size image](#)

Fig. 3. Detrended [correspondence analysis](#) (DCA) of identified OTUs from 16S rRNA genes [sequencing](#)(a), all functional genes (b), *gyrB* genes (c) and [electron transfer](#) related genes (d) detected from GeoChip [hybridization](#).

3.5. Unique functional genes and microbial diversity indices

A total of 1067 functional genes (accounting for 2.20% of all detected functional genes) absolutely undetected in the S25-biocathode but detected at least in three 10-biocathodes. Moreover, the 10-biocathode enriched 101 unique functional genes that were completely absent in the S25-biocathode. A total of 2213 functional genes (accounting for 4.57%) absolutely undetected in the 10-biocathode but detected at least in the three S25-biocathodes. Moreover, the S25-biocathode enriched 208 unique functional genes that were completely absent in the 10-biocathode. These unique functional genes mainly belongs to carbon cycling, metal resistance, stress and organic pollutants [bioremediation](#) gene categories (relative abundance >10%) ([Fig. S4](#)). The temperature elevation did not significantly altered the phylogenetic diversity based on the richness, *H* and *1/D* indices, though the S25-biocathode had a relatively higher richness and lower *H* and *1/D* indices than those of the 10-biocathode. The temperature elevation significantly increased the functional gene diversity based on the detected functional genes numbers and abundances ($P \leq 0.07$) ([Table S2](#)). Additionally, the temperature elevation slightly decreased the Chao1 value of the S25-biocathode (1352 ± 317) compared to the 10-biocathode (1416 ± 373). These results indicated that the temperature elevation relatively increased the richness (OTUs and functional gene numbers) and obviously enriched unique functional genes in the biocathode communities, which fitted the general regularity that more microbial species are likely to live at ambient temperature.

3.6. Differences of biocathode communities structure at phylum and class levels

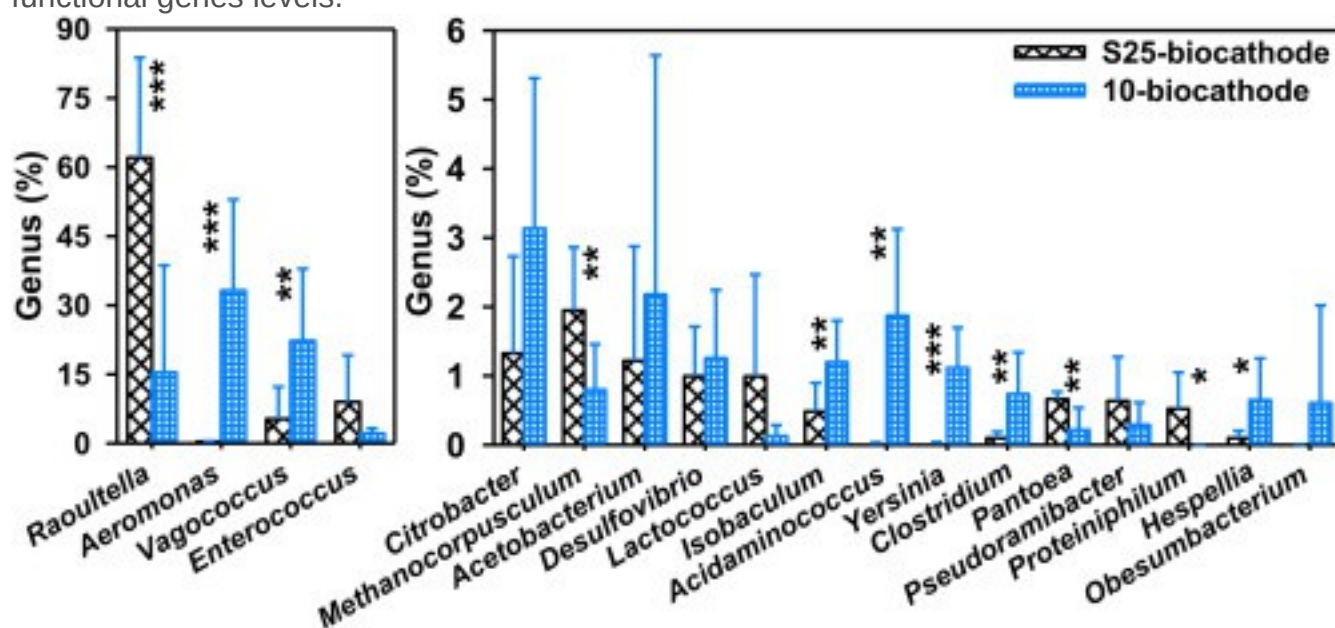
A total of 18 phyla were identified in the 12 biocathodes, therein 3 dominant phyla including *Proteobacteria*, *Firmicutes* and *Bacteroidetes* that frequently appeared in [electrode microbial communities](#) were not significantly differed between the two biocathode groups. The relative abundances for *Proteobacteria* (from 61.39 ± 22.86 to $69.30 \pm 18.54\%$; $P = 0.526$), *Bacteroidetes* (from 1.43 ± 0.37 to $2.36 \pm 2.04\%$; $P = 0.322$), *Euryarchaeota* (from 0.81 ± 0.67 to $2.74 \pm 2.38\%$; $P = 0.105$) and other classified and unclassified phyla (from 0.28 ± 0.11 to

1.62 ± 1.06%; $P = 0.026$) were relatively increased after the temperature elevation. The 10-biocathode had a relatively higher abundance of *Firmicutes* (36.10 ± 23.02%) than that of the S25-biocathode (23.98 ± 14.20%; $P = 0.303$). A total of 33 classes were classified in the 12 biocathodes and the most of the sequences belonging to 6 classes (relative abundance >1%). Gram-positive *Bacilli* and *Clostridia* species were relatively enriched in the 10-biocathode compared to those in the S25-biocathode, while *Gammaproteobacteria*, *Bacteroidia* and other classified and unclassified classes were relatively increased excepting *Methanomicrobia* species were significantly enriched (from 0.80 ± 0.66 to 1.95 ± 0.91%; $P = 0.034$) in the S25-biocathode (Fig. S5).

3.7. The potential function of dominant genera

A total of 182 genera were classified among the 12 biocathodes. Eighteen genera with relative abundance >0.5% were shown in Fig. 4. *Aeromonas* (33.16 ± 19.82%; $P = 0.01$) and *Vagococcus* (22.25 ± 15.67%; $P = 0.046$) were significantly enriched under 10 °C, which was consistent with the cold-adapted ability of them (Rouf and Rigney, 1971, Teixeira et al., 1997). Electrochemically active *Aeromonas* was capable of reducing nitroaromatics 1-nitropyrene to aromatic amine 1-aminopyrene (Kinouchi et al., 1982, Pham et al., 2003). *Vagococcus* was capable of biodegrading *p*-chloronitrobenzene (Bao et al., 2009). Importantly, the relative abundances of *Aeromonas* ($r = -0.79$, $P = 0.019$) and *Vagococcus* ($r = -0.66$, $P = 0.075$) showed a significant negative correlation to the maximal AMCl₂ yield under the opened circuit mode (pure anaerobic bioreduction). This result strongly suggests that the low temperature acclimation with electrical stimulation enhanced the CAP nitro group reduction with dominant cold-adapted nitroreductase-carrying bacteria under 10 °C. *Raoultella* (62.06 ± 21.72%; $P = 0.005$) and *Enterococcus* (9.00 ± 10.16%) obviously or relatively enriched in the S25-biocathode attributed to the fact that they could reduce nitroaromatics into corresponding aromatic amines with glucose as electron donor (Claus et al., 2007, Rafii et al., 2003). Factually, the relative abundance of *Raoultella* showed a significant positive correlation to the maximal AMCl₂ yield ($r = 0.81$, $P = 0.014$) under the opened circuit mode. Other dominant genera (0.52–3.13%) including *Citrobacter*, *Acetobacterium*, *Desulfovibrio*, *Isobaculum* ($P = 0.042$), *Yersinia* ($P = 0.006$), *Acidaminococcus* ($P = 0.015$), *Clostridium* ($P = 0.050$), *Hespellia* ($P = 0.078$) and *Obesumbacterium* were relatively or significantly enriched in the 10-biocathode. Among these dominant genera, *Citrobacter*, *Desulfovibrio* and *Clostridium* were able to

reduce nitroaromatics (e.g., 1-nitropyrene, CAP and nitrobenzene) into corresponding aromatic amines ([Howard et al., 1983](#), [Spain, 1995](#)). While relative abundances of *Methanocorpusculum* ($P = 0.034$), *Lactococcus*, *Pantoea* ($P = 0.017$), *Pseudoramibacter* and *Proteiniphilum* ($P = 0.060$) were relatively or obviously increased in the S25-biocathode. The enrichment of *Methanocorpusculum* in the S25-biocathode was consistent with the fact that low temperature could inhibit the [methanogen](#) metabolic activity ([Lu et al., 2011](#)). GeoChip analysis further indicated that the [methane](#) production gene *mcrA* ($P = 0.032$) abundances in the 10-biocathode was significantly lower than that of the S25-biocathode, which showed the same trend both at 16S rRNA and functional genes levels.



1. [Download high-res image \(441KB\)](#)
2. [Download full-size image](#)

Fig. 4. The dominant genera in the 10-biocathode and S25-biocathode communities.

***, ** and * denotes significance at 0.01, 0.05, and 0.10 test levels, respectively.

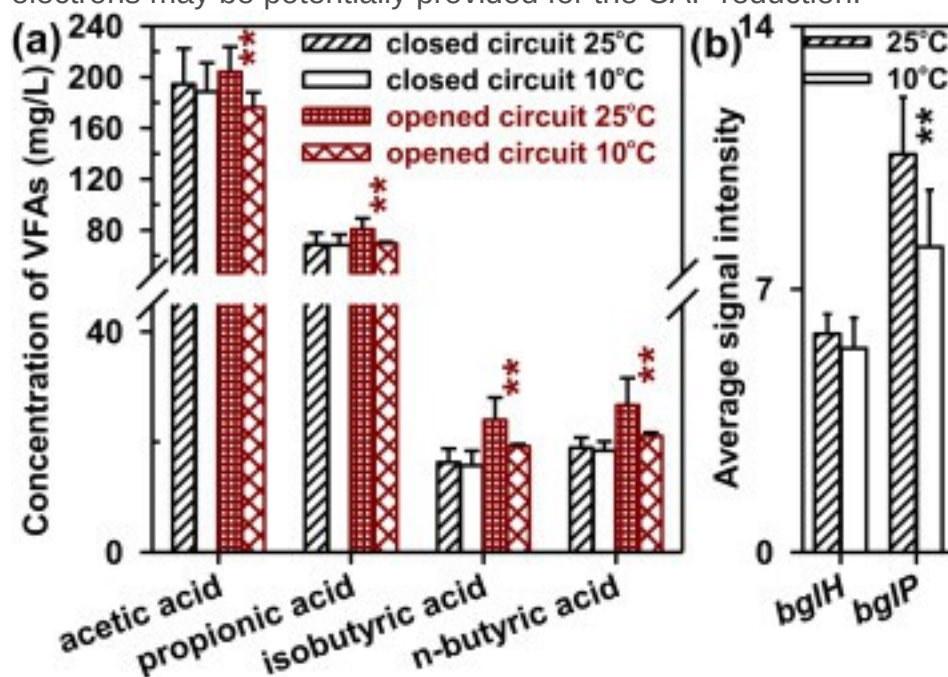
Based on the phylogenetically identified known nitroaromatics-metabolizing and electrochemically active taxa, the potential function of these dominant genera mentioned above was revealed as following. Firstly, most of the dominant genera (*Aeromonas*, *Raoultella*, *Enterococcus*, *Citrobacter*, *Desulfovibrio* and *Clostridium*) are capable of reducing nitroaromatics to corresponding aromatic amines or [biodegradation](#) of nitroaromatics (*Vagococcus*) ([Bao et al., 2009](#), [Howard et al., 1983](#), [Kinouchi et al., 1982](#), [Liang et al., 2014](#), [Spain, 1995](#)). Subsequently, most of the dominant genera were identified with electrochemical activity (*Aeromonas*, *Citrobacter*, *Lactococcus*, *Desulfovibrio* and *Clostridium*) ([Kumar et al.,](#)

2015, Logan, 2009) or dominated in biocathode communities (*Raoultella* and *Enterococcus*) (Liang et al., 2014, Wang et al., 2011). However, the demonstration of the biocathodic electrochemical activity of diverse dominant electrochemically active species with nitroaromatics as electron acceptor is needed. Finally, *Aeromonas* and *Vagococcus* with the cold-adapted feature were markedly enriched in the 10-biocathode. Additionally, *Acidaminococcus* and *Clostridium* were also obviously enriched in the 10-biocathode ($P < 0.05$) (Fig. 4). A recent study indicated that *Acidaminococcus* (1.1%) and *Clostridium* (6.2%) were enriched in a 10°C-performed *p*-fluronitrobenzene-mineralizing biocathode community (Zhang et al., 2015b). Dominant functional species were selectively enriched by the continuous electrical stimulation at two temperatures respectively, which likely involved in the stress response to the low temperature acclimation and environmental temperature perturbations and finally played a critical role for maintaining the CAP reduction and electron transfer functions stability.

3.8. Genes involved in glucose transport and metabolism

Microbial metabolism of [carbohydrate](#) glucose could release the intracellular electrons for the enhanced reduction of nitroaromatics (e.g., [nitrobenzene](#) and CAP) within biocathode communities (Liang et al., 2013, Liang et al., 2014, Wang et al., 2011). Four main volatile [fatty acids](#) (VFAs) accumulated from the biocathodic glucose metabolism were not obviously differed between the two temperature groups under the closed circuit mode, while the 10-biocathode accumulated significantly lower VFAs content (at 6th h) than those of the S25-biocathode without the electrical stimulation ($P < 0.05$) (Fig. 5), which was in accord with that more glucose was unconsumed in the opened circuit 10-biocathode (90.54 ± 3.97 mg/L) than that in the opened circuit S25-biocathode (37.04 ± 1.14 mg/L). For the functional genes level, 6 β -glucosidase genes (*bglH*) belonging to the glycosyl hydrolase family 1, which involves in the bacterial carbohydrate transport and metabolism, were detected in the biocathode communities. The intensity of a *bglH* from *Pectobacterium atrosepticum* SCRI1043 (50123305) was significantly increased ($P = 0.061$) in the 10-biocathode, while the total abundances of *bglH* in the biocathode communities were not significantly differed before and after the temperature elevation. The bacterial phosphoenolpyruvate: sugar phosphotransferase system (PTS) is a multi-protein system involves in the regulation of a variety of metabolic and transcriptional processes, which is necessary for the uptake of carbohydrates across the cytoplasmic membrane and their [phosphorylation](#). The total abundances of 16 PTS beta-glucoside [transporter](#) subunit II ABC component (*bglP*)

genes from 9 genera were markedly enriched in the S25-biocathode than those of the 10-biocathode ($P = 0.033$) (Fig. 5). Three *bglP* genes from *Bacillus halodurans* C-125 (10173209), *Bacillus licheniformis* ATCC 14580 (52350379) and *Anaerostipes caccae* DSM 14662 (16765266) were unique in the S25-biocathode. Five *bglH* and 12 *bglP* genes came from Gram-positive genera (e.g., *Anaerostipes*, *Bacillus*, *Clostridium* and *Lactobacillus*) in *Firmicutes*. Factually, *bglP* abundances showed a significant positive correlation to the measured [propionic acid](#), isobutyric acid and n-butyric acid contents at 6th h ($r = 0.55$ – 0.60 , $P < 0.10$) as well as [acetic acid](#) and isobutyric acid contents at 24th h ($r = 0.62$ – 0.63 , $P < 0.06$) of the opened circuit mode, and isobutyric acid content (at 6th h, closed circuit) ($r = 0.69$, $P = 0.027$). Thus, the electrical stimulation could counteract the difference in glucose metabolism under 10 °C. These results indicated that the electrical stimulation could improve the glucose metabolism on the 10-biocathode, and additional electrons may be potentially provided for the CAP reduction.



1. [Download high-res image \(436KB\)](#)
2. [Download full-size image](#)

Fig. 5. Comparison of the VFAs accumulation from intracellular electron donor [glucose fermentation](#) (a) as well as the glucose transport and metabolism genes signal intensity (b) of the biocathode communities under constant 10 °C and switched 25 °C.

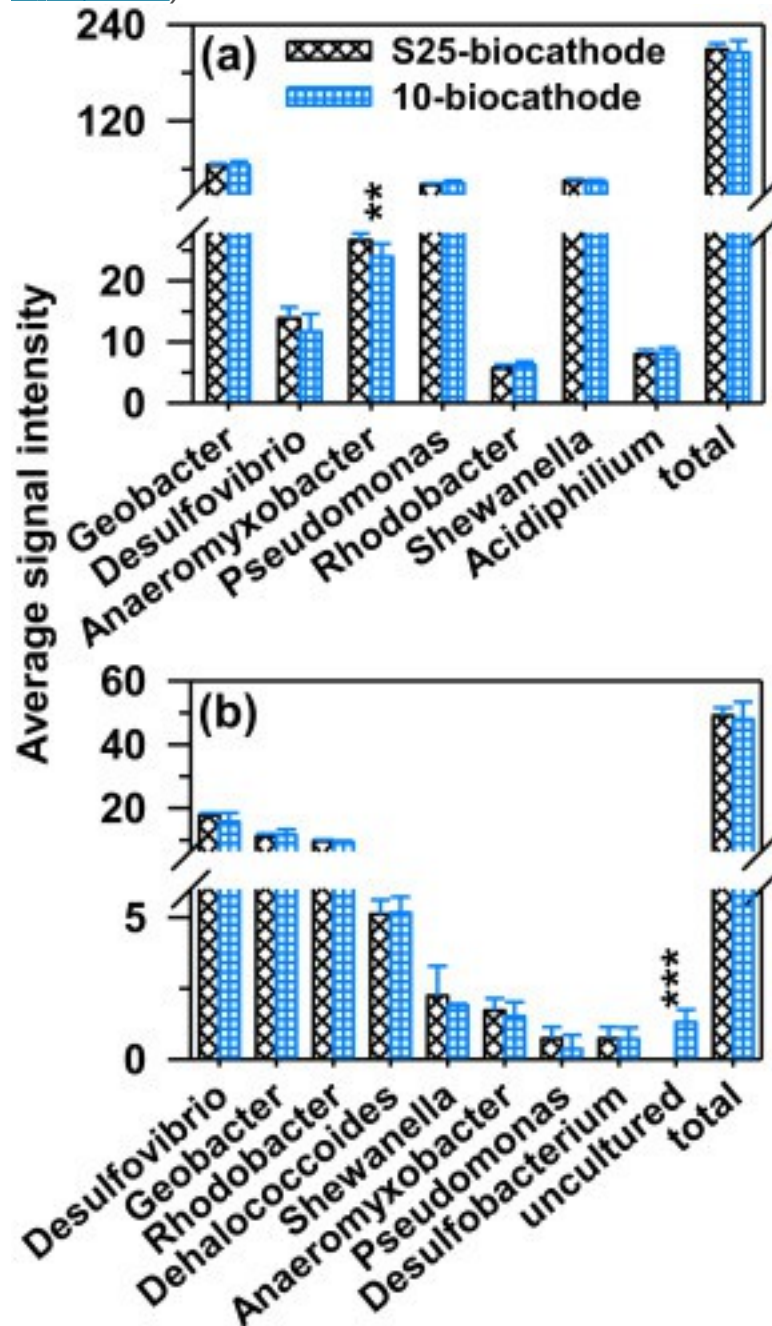
3.9. Genes involved in cathode biofilm formation

The extracellular type IV pilin and polymeric substances (EPS) networks have a key role in [biofilm](#) formation and adherence to [solid surfaces](#) ([Flemming and Wingender, 2010](#), [Giltner et al., 2012](#)). The total gene abundances of pilin ($P = 0.205$) and EPS synthesis ($P = 0.514$) were not significantly differed between the two biocathode groups ([Fig. S6](#)), and such a phenomenon was in accord with the fact that biocathode communities had comparative total cathodophilic microbes (both high and low growth activity cells) before and after the temperature elevation.

3.10. Genes involved in electron transfer

Cytochrome *c* proteins are essential for electron transfer in dissimilatory anaerobic respiration of extracellular electrons acceptors ([Lovley, 2012](#), [Richter et al., 2012](#), [Sydow et al., 2014](#)) and it is also the case for the reversed electron transfer pathway for intracellular reductive metabolism using electrode as electron donor ([Beese-Vasbender et al., 2015](#), [Dantas et al., 2015](#), [Okamoto et al., 2014](#), [Ross et al., 2011](#), [Wang et al., 2015](#)). In the current study, a total of 256 cytochrome *c* genes from 7 electrochemically active genera (*Geobacter*, *Anaeromyxobacter*, *Shewanella*, [Pseudomonas](#), *Desulfovibrio*, *Acidiphilium* and *Rhodobacter*) were detected ([Hasan et al., 2013](#), [Logan, 2009](#), [Strycharz et al., 2010](#)). Additionally, other 4 cytochrome *c* genes from *Sulfolobus tokodaii* (15623162) and *Metallosphaera sedula* (145701515, 145701603 and 145703030) were also detected. The total signal intensities for cytochrome *c* genes from *Anaeromyxobacter* were significantly enriched in the S25-biocathode ($P = 0.046$). However, the total signal intensities for cytochrome *c* genes from other 6 genera and the sum total intensities were not significantly differed between the two biocathode groups ([Fig. 6a](#)). Concretely, the 10-biocathode and S25-biocathode both enriched 6 unique cytochrome *c* genes, respectively (at least from 3 biocathodes but were completely absent in the opposite biocathodes). The unique enriched cytochrome *c* genes are rich in heme-binding sites, which might act as a [capacitor](#) and play an essential role in extracellular electron transport ([Pokkuluri et al., 2011](#)). Interestingly, a cytochrome *c* carrying 27 heme-binding sites from *Geobacter sulfurreducens* PCA (39997308) was unique in the 10-biocathode. Two periplasmic cytochrome *c* belonging to DmsE family in *Geobacter bemidjensis* Bem (197086873 and 197086874) contained 26 and 16 heme-binding sites, respectively, which were unique in the 10-biocathode. While a decaheme DmsE cytochrome *c* from *Anaeromyxobacter* sp. Fw109-5 (153005942) was unique in the S25-biocathode. Additionally, 10 and 15 cytochrome *c* genes were marginally ($P < 0.10$) enriched in the 10-biocathode and S25-

biocathode, respectively. Two outer membrane cytochrome *c* genes *omcX* and *omcA/mtrC* (39995776 and 120598319) were particularly enriched ($P < 0.02$) in the S25-biocathode (Fig. S7). Outer-membrane cytochrome *c* OmcA of *Shewanella oneidensis* MR-1 has been functionally proved to be able to [capture electrons](#) from a cathode to proceed reductive metabolism (Okamoto et al., 2014).



1. [Download high-res image \(639KB\)](#)
2. [Download full-size image](#)

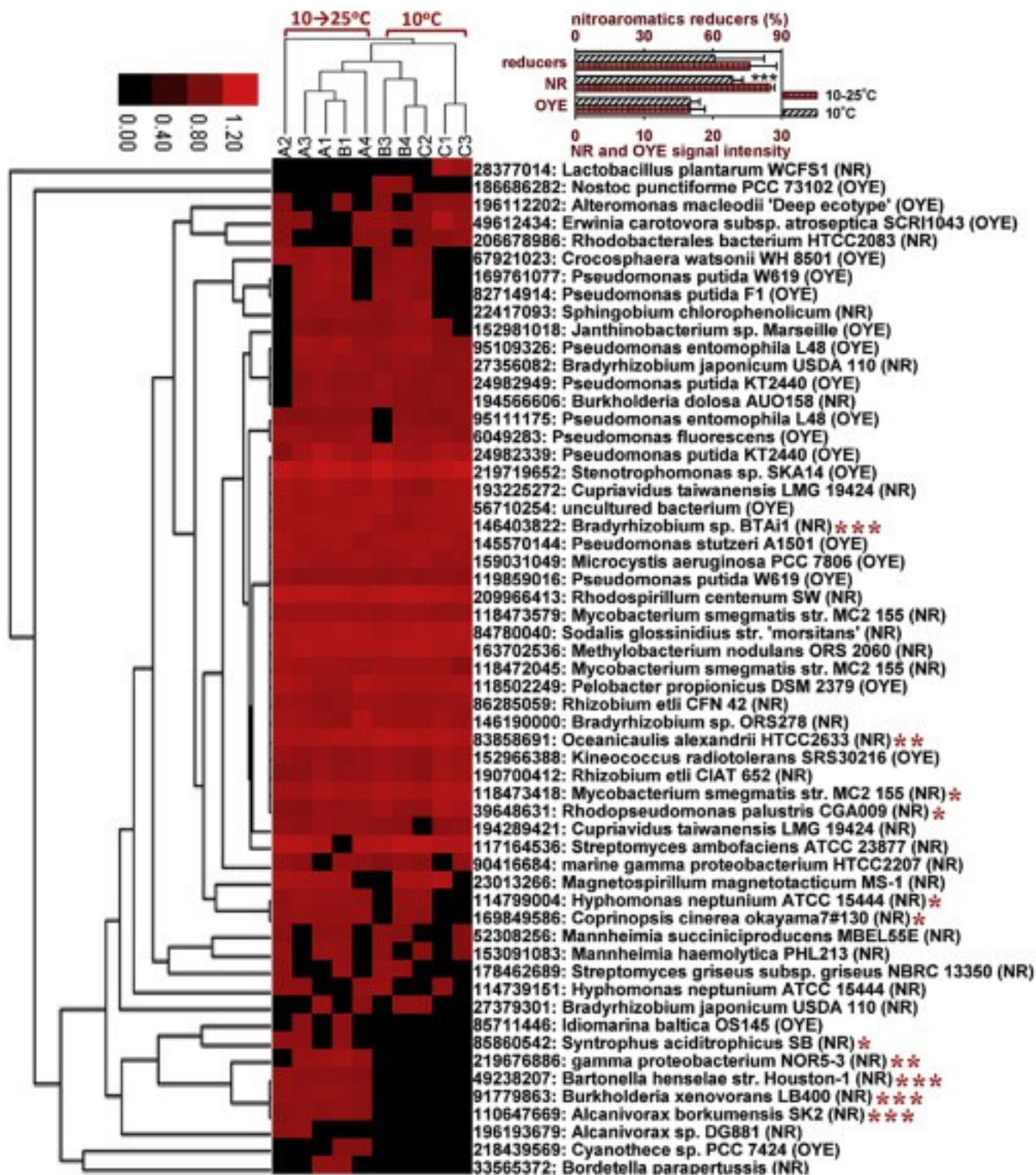
Fig. 6. Comparison of the signal intensity of key [electron transfer cytochrome c](#) (a) and hydrogenase genes (b) from the 10-biocathode and S25-biocathode communities. Hydrogenases have been involved in electron flow for reductive metabolism in biocathode ([Aulenta et al., 2008](#), [Caffrey et al., 2008](#), [Deutzmann et al., 2015](#)). In the current study, a total of 65 hydrogenase genes from 8 genera and 2 uncultured microorganisms were detected, 23 of which came from *Desulfovibrio* species that with bifunctional features of nitroaromatics reduction and electrochemical activity. The total signal intensities for hydrogenase genes from uncultured microorganisms were significantly enriched in the 10-biocathode ($P = 0.003$). Concretely, 2 hydrogenase genes came from *Dehalococcoides* sp. GT ($P = 0.093$; 269920284) and *Desulfovibrio desulfuricans* G20 ($P = 0.018$; 78357178) were enriched in the 10-biocathode, while 6 *Desulfovibrio* and *Rhodobacter* species carrying hydrogenase genes were enriched ($P < 0.09$) in the S25-biocathode. The 10-biocathode and S25-biocathode both enriched 3 unique hydrogenase genes, respectively ([Fig. S6](#)). However, the total signal intensities for hydrogenase genes from 8 genera respectively and the sum total intensities were not significantly differed between the two biocathode groups ([Fig. 6b](#)). The low temperature acclimation and temperature elevation selectively enriched different cytochrome *c* and hydrogenase genes, especially in the S25-biocathode ([Fig. S7](#)). The total intensities of important electron transfer related cytochrome *c* and hydrogenase genes were not significantly differed before and after the temperature elevation for maintaining electron transfer efficiency during the bioelectrochemical CAP reduction.

Partial electrons from cathode and glucose metabolism could be captured by cathodophilic microbes within biocathode to proceed energy metabolism. A total of 65 related genes to electron transport respiratory chain (excepting for cytochrome *c* genes) including 4Fe-4S ferredoxin, Fe-S cluster binding protein, NADH quinone/ubiquinone oxidoreductase, cytochrome *b*, [ATP](#) synthase (adenosine triphosphate synthase) and ferredoxin_oxidoreductase were detected in the biocathode communities. The abundances of these genes in the biocathode communities were shown in [Fig. S8](#). Only cytochrome *b* gene showed significant higher abundances in the 10-biocathode ($P = 0.072$), while other electron transport respiratory related genes showed no obvious differences between the two biocathode groups. *Metallosphaera sedula* DSM 5348 carrying cytochrome *b* gene (145701356) was unique in the 10-biocathode. Collectively, like ferredoxin, Fe-S cluster binding protein, NADH [quinone](#) oxidoreductase, ATP synthase, outer membrane and periplasmic cytochrome *c* as well as hydrogenase genes were detected in the current study, indicating their involvement in the

biocathodic [electron transfer and energy](#) conservation ([Choi and Sang, 2016](#), [Kim et al., 2015](#), [Kracke et al., 2015](#)).

3.11. Genes involved in nitroaromatics reduction

NAD(P)H dependent nitroreductase (NR), NADPH dependent old yellow [enzyme](#) (OYE) like FMN and NADPH dependent cytochrome P450 reductase are capable of reducing nitroaromatics to the corresponding aromatic amines ([Roldan et al., 2008](#), [Spain, 1995](#)). NR could be involved in the bioelectrochemical reduction of nitroaromatics as the measured midpoint potential of NR and OYE cofactors (-0.19 and -0.23 V vs SHE, respectively) are thermodynamically favorable ([Koder et al., 2002](#), [Stewart and Massey, 1985](#)) comparing to the nitroaromatics reduction potential that observed from the CV analysis in previous reports ([Liang et al., 2014](#), [Wang et al., 2011](#)) and this study. Hierarchical clustering analysis of the NR and OYE genes showed that the 10-biocathode communities were separated from the S25-biocathode communities ([Fig. 7](#)). The total abundance of NR genes were significantly enriched in the S25-biocathode ($P = 0.0004$), which accorded with that the S25-biocathode ($75.99 \pm 11.75\%$) enriched relatively higher abundances of nitroaromatics reducers (belong to 23 genera) than those of the 10-biocathode ($60.51 \pm 21.74\%$) ([Table S3](#)). The significant higher AMCl_2 yield in the opened circuit S25-biocathode that significantly positively correlated with the higher NR abundances ($r = 0.90$, $P = 0.002$). Specifically, 3 NR genes came from *Alcanivorax borkumensis* SK2 (110647669), *Bartonella henselae* str. Houston-1 (49238207) and *Burkholderia xenovorans* LB400 (91779863) were unique in the five S25-biocathode communities. Other 4 NR genes (85860542, 219676886, 33565372 and 196193679) were undetected in the 10-biocathode while enriched in at least two S25-biocathode communities. *Lactobacillus plantarum* WCFS1 carrying NR gene (28377014) was unique in the two 10-biocathode communities. The OYE genes carrying bacteria, *Idiomarina baltica* OS145 (85711446) and *Cyanothece* sp. PCC 7424 (218439569), were only found in the two S25-biocathode communities. While the other OYE gene (186686282) carrying bacteria, *Nostoc punctiforme* PCC 73102 was enriched in the two 10-biocathode communities ([Fig. 7](#)). The total abundance of OYE genes was not significantly differed between the two biocathode groups. Only one NADPH dependent cytochrome P450 reductase gene (134100738) from *Saccharopolyspora erythraea* was detected in the biocathode communities, showing significantly higher abundance in the 10-biocathode ($P = 0.056$).



1. [Download high-res image \(1MB\)](#)
2. [Download full-size image](#)

Fig. 7. Hierarchical clustering of nitroreductase (NR) and old yellow enzyme (OYE) genes from the 10-biocathode and S25-biocathode communities. The inset histogram

indicated the total abundance for each gene family and [relative abundance](#) of nitroaromatics reducers. The significant differences of each gene signal intensity between the two biocathode groups were also shown.

[Sulfite](#) reductase from *Desulfovibrio* sp. is responsible for the reduction of aromatic [hydroxylamines](#) to the corresponding aromatic amines ([Spain, 1995](#)). Twenty two sulfite reductase A subunit (*dsrA*) and 16 sulfite reductase B subunit (*dsrB*) genes from *Desulfovibrio* species were detected in the biocathode communities. The total abundances of *dsrA* and *dsrB* genes were not obviously differed between the two biocathode groups, which was consistent with the similar trend of the relative abundance of *Desulfovibrio* sp. at taxonomic 16S rRNA gene level.

Interestingly, *dsrA* (107784967) and *dsrB* (10279674) genes from the same *Desulfovibrio desulfuricans* were both significantly enriched in the 10-biocathode communities ($P < 0.04$). Other 5 *dsrAB* genes had a marginally higher abundances in either the S25-biocathode or the 10-biocathode ($P < 0.10$) were also shown in [Fig. S9](#).

[Carbon monoxide dehydrogenase](#) (CODH) belongs to *Desulfovibrio* and *Clostridium* species are capable of reducing nitroaromatics to the corresponding aromatic hydroxylamines ([Spain, 1995](#)). Five CODH genes from *Clostridium* sp. and 2 CODH genes from *Desulfovibrio* were detected in the biocathode communities. The *Clostridium* carrying CODH genes showed significant higher abundance in the S25-biocathode ($P = 0.007$), while the *Desulfovibrio* CODH genes showed no significant difference between the two biocathode groups.

Collectively, the temperature elevation obviously enriched related genes involved in nitroaromatics reduction in the S25-biocathode, while the low temperature acclimation with electrical stimulation selectively enriched specific functional genes and sufficient nitroaromatics reducers associated with nitroaromatics reduction to guarantee overall reduction efficiency in the 10-biocathode.

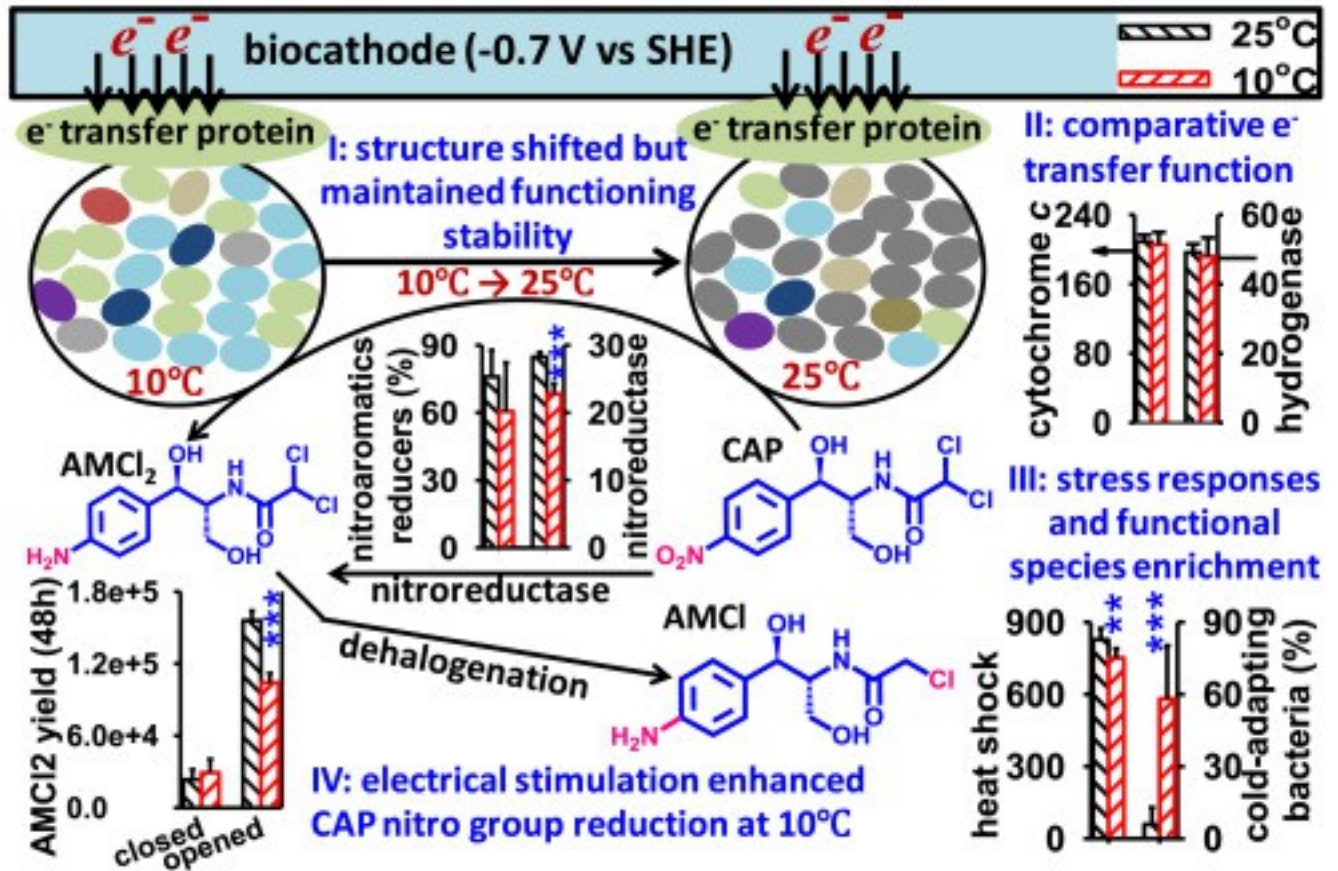
3.12. Genes involved in heat shock response

Regulatory gene *hrcA* and chaperon machinery genes *dnaK*, *grpE*, *groES*, and *groEL* are involved in [heat shock](#) responses ([Zhou et al., 2013](#)). Sigma factors are the key players in the transcription initiation of functional [gene expression](#) in [prokaryotes](#) ([Feklistov et al., 2014](#)), while sigma factors σ^{32} (RpoH) and σ^{24} (RpoE) are also involved in heat shock response ([Zhou et al., 2013](#)). The total abundances of *hrcA* ($P = 0.022$), *groES* ($P = 0.027$), $\sigma^{24}RpoE$ ($P = 0.031$) and $\sigma^{32}RpoH$ ($P = 0.10$) in the biocathode communities were significantly or marginally enriched after the temperature elevation. The total abundances of other 3 heat shock

response genes *dnaK*, *grpE* and *groEL* were relatively increased in the S25-biocathode. The total of 5 heat shock response genes showed obviously higher abundances in the S25-biocathode ($P = 0.014$). Other 2 [RNA](#) polymerase sigma factors $\sigma^{38}RpoS$ ($P = 0.035$) and $\sigma^{70}RpoD$ ($P = 0.053$) were also markedly enriched in the S25-biocathode ([Fig. S10](#)). Concretely, 2 *hrcA* and 3 $\sigma^{24}RpoE$ genes belongs to *Beijerinckia indica* (182678250), *Alicyclobacillus acidocaldarius* (257478691), Opitutaceae [bacterium](#)TAV2 (224803786), *Solibacter usitatus* Ellin6076 (116626963) and *Dickeya zeae* Ech1591 (247537313) were detected in the S25-biocathode, but they were completely absent in the 10-biocathode. Collectively, genes related to heat shock response protein were significantly enriched in the S25-biocathode, indicating that the stress genes likely involved in maintaining the biocathode communities functioning stability upon the temperature elevation.

3.13. A concept model for the biocathode functioning stability under low temperature

Understanding the improvement mechanisms of the low temperature acclimation with continuous electrical stimulation on the biocathode functioning stability is critical to accelerate [refractory](#) environmental pollutants [detoxification](#) in cold regions. Based on the data from GeoChip [hybridization](#), 16S rRNA gene Illumina [sequencing](#), [chemical kinetics](#) and bioelectrochemistry, we proposed a concept model for the effects of the low temperature acclimation with electrical stimulation on the functioning stability of complicated biocathode communities for CAP detoxification ([Fig. 8](#)).



1. [Download high-res image \(877KB\)](#)
2. [Download full-size image](#)

Fig. 8. A concept model for the effects of the low temperature [acclimation](#) with continuous electrical stimulation on the functioning stability of biocathode communities for CAP [detoxification](#).

First, the 10-biocathode and S25-biocathode both enriched core functional community respectively. The temperature elevation significantly altered the 10-biocathode [communities structure and composition](#). The CAP degradation and products formation dynamics indicated that the 10-biocathode had comparative catalyzed capability compared to the S25-biocathode, though the low temperature significantly decreased the terminal AMCl product generation rate but not the $Y_{\max-AMCl}$ in the 10-biocathode. Second, the important function between the cathode surface and the formed biofilm is the electron flow capability. The total abundances of 2 important electron transfer genes (cytochrome c and hydrogenase) showed no significant differences between the 10-biocathode and S25-biocathode, which accorded with the 10-biocathode and S25-biocathode had comparative charge accumulation during CAP reduction ([Fig. 1f](#)) and nearly the same CV catalyzed feature ([Fig. S2](#)). The comparative

electron transfer function lay a critical foundation for maintaining the functioning stability of the bioelectrochemical CAP reduction under constant low temperature. Finally, the 10-biocathode and S25-biocathode selectively enriched 61–76% nitroaromatics reducers. The 10-biocathode dominated by the potential cold-adapted nitroaromatics-biodegrading bacteria ($58.06 \pm 22.14\%$), while the S25-biocathode significantly enriched the heat shock response genes abundance and nitroaromatics reducers ($75.99 \pm 11.75\%$) simultaneously after the temperature elevation. The significantly higher AMCl_2 yield in the opened circuit S25-biocathode positively correlated with the obvious higher nitroreductase gene abundance. This could explain why the closed circuit S25-biocathode had a significantly greater k_{AMCl_2} ($P = 0.002$) and lower AMCl_2 yield between 12 and 24 h ($P < 0.0006$) than those of the closed circuit 10-biocathode. Collectively, the low temperature acclimation with continuous electrical stimulation obviously increased the CAP nitro group reduction efficiency and functioning stability of biocathode communities mainly through selectively enriching cold-adapted functional species, co-existing metabolically similar nitroaromatics reducers and maintaining the relative abundance of key electrons transfer genes (e.g., cytochrome *c* and hydrogenase). For the potential applications in cold environments, this study provides a new strategy to increase the functioning stability of biocathode communities for accelerating environmental pollutants treatment in wastewater system. Moreover, the cold-adapted biocathode system could save a lot during wastewater heating process and show a more adaptive ability to environmental temperature changes than the ambient temperature enriched biocathode communities.

4. Conclusions

This study demonstrated that the low temperature [acclimation](#) with electrical stimulation enhanced the 10-biocathode communities functioning stability for CAP [reduction](#) especially for the nitro group reduction process. The 10-biocathode functioning stability maintained mainly through selectively enriching cold-adapted functional species, coexisting metabolically similar nitroaromatics reducers and maintaining the [relative abundance](#) of key [electron transfer](#) genes. The current study provides new insights into biocathode functioning stability for accelerating environmental pollutants treatment in cold [wastewater](#) system from [phylogenetic](#) and functional genes perspectives, which would enlarge the potential applications of bioelectrochemical technology for [refractory antibiotic wastewaters treatment](#) in cold regions.

Acknowledgment

This work was supported by the National Science Foundation for Distinguished Young Scholars of China (No. [51225802](#)), the National Natural Science Foundation of China (No. [31500084](#)) and the Hundred Talents Program of the Chinese Academy of Sciences (No. [29BR2013001](#)).

Appendix A. Supplementary data

The following is the supplementary data related to this article:

[Download Word document \(3MB\)Help with docx files](#)

References

[Andersson and Hughes, 2014](#)

D.I. Andersson, D. Hughes **Microbiological effects of sublethal levels of antibiotics**
Nat. Rev. Microbiol., 12 (7) (2014), pp. 465-478

[CrossRefView Record in Scopus](#)

[Aulenta et al., 2008](#)

F. Aulenta, A. Canosa, M. Majone, S. Panero, P. Reale, S. Rossetti **Trichloroethene dechlorination and H₂ evolution are alternative biological pathways of electric charge utilization by a dechlorinating culture in a bioelectrochemical system**
Environ. Sci. Technol., 42 (16) (2008), pp. 6185-6190

[CrossRefView Record in Scopus](#)

[Bao et al., 2009](#)

H.Y. Bao, J. Gao, Y.X. Liu, Y.J. Su **A study of biodegradation/gamma-irradiation on the degradation of p-chloronitrobenzene**
Radiat. Phys. Chem., 78 (12) (2009), pp. 1137-1139

[ArticleDownload PDFView Record in Scopus](#)

[Beese-Vasbender et al., 2015](#)

P.F. Beese-Vasbender, S. Nayak, A. Erbe, M. Stratmann, K.J.J. Mayrhofer **Electrochemical characterization of direct electron uptake in electrical microbially influenced corrosion of iron by the lithoautotrophic SRB *Desulfopila corrodens* strain IS4**
Electrochim. Acta, 167 (2015), pp. 321-329

[ArticleDownload PDFView Record in Scopus](#)

[Caffrey et al., 2008](#)

S.M. Caffrey, H.S. Park, J. Been, P. Gordon, C.W. Sensen, G. Voordouw **Gene expression by the sulfate-reducing bacterium *Desulfovibrio vulgaris* Hildenborough grown on an iron electrode under cathodic protection conditions**
Appl. Environ. Microbiol., 74 (8) (2008), pp. 2404-2413

[CrossRefView Record in Scopus](#)

[Choi and Sang, 2016](#)

O. Choi, B.I. Sang **Extracellular electron transfer from cathode to microbes: application for biofuel production**

Biotechnol. Biofuels, 9 (2016), p. 11, [10.1186/s13068-016-0426-0](https://doi.org/10.1186/s13068-016-0426-0)

[CrossRefView Record in Scopus](#)

[Claus et al., 2007](#)

H. Claus, N. Perret, T. Bausinger, G. Fels, J. Preuss, H. König **TNT transformation products are affected by the growth conditions of *Raoultella terrigena***

Biotechnol. Lett., 29 (3) (2007), pp. 411-419

[CrossRefView Record in Scopus](#)

[D'Amico et al., 2006](#)

S. D'Amico, T. Collins, J.C. Marx, G. Feller, C. Gerday **Psychrophilic microorganisms: challenges for life**

EMBO Rep., 7 (4) (2006), pp. 385-389

[CrossRefView Record in Scopus](#)

[Dantas et al., 2015](#)

J.M. Dantas, L.M. Campelo, N.E. Duke, C.A. Salgueiro, P.R. Pokkuluri **The structure of PccH from *Geobacter sulfurreducens*-a novel low reduction potential monoheme cytochrome essential for accepting electrons from an electrode**

FEBS J., 282 (11) (2015), pp. 2215-2231

[CrossRefView Record in Scopus](#)

[Deutzmann et al., 2015](#)

J.S. Deutzmann, M. Sahin, A.M. Spormann **Extracellular enzymes facilitate electron uptake in biocorrosion and bioelectrosynthesis**

mBio, 6 (2) (2015), pp. e00496-15, [10.1128/mBio.00496-15](https://doi.org/10.1128/mBio.00496-15)

[View Record in Scopus](#)

[Feklistov et al., 2014](#)

A. Feklistov, B.D. Sharon, S.A. Darst, C.A. Gross **Bacterial sigma factors: a historical, structural, and genomic perspective**

Annu. Rev. Microbiol., 68 (2014), pp. 357-376

[CrossRefView Record in Scopus](#)

[Feng et al.,](#)

[2015](#)

H. Feng, X. Zhang, K. Guo, E. Vaiopoulou, D. Shen, Y. Long, J. Yin, M. Wang **Electrical stimulation improves microbial salinity resistance and organofluorine removal in bioelectrochemical systems**

Appl. Environ. Microbiol., 81 (11) (2015), pp. 3737-3744

[CrossRefView Record in Scopus](#)

[Flemmi](#)

[ng and](#)

[Wingender, 2010](#)

H.C. Flemming, J. Wingender **The biofilm matrix**

Nat. Rev. Microbiol., 8 (9) (2010), pp. 623-633

[View Record in Scopus](#)

[Giltner et al., 2012](#)

C.L. Giltner, Y. Nguyen, L.L. Burrows **Type IV pilin proteins: versatile molecular modules**

Microbiol. Mol. Biol. Rev., 76 (4) (2012), pp. 740-772

[CrossRefView Record in Scopus](#)

[Hasan et al., 2013](#)

K. Hasan, S.A. Patil, K. Gorecki, D. Leech, C. Hagerhall, L. Gorton **Electrochemical communication between heterotrophically grown *Rhodobacter capsulatus* with electrodes mediated by an osmium redox polymer**

Bioelectrochemistry, 93 (2013), pp. 30-36

[ArticleDownload PDFView Record in Scopus](#)

[He et al., 2010](#)

Z.L. He, Y. Deng, J.D. Van Nostrand, Q.C. Tu, M.Y. Xu, C.L. Hemme, X.Y. Li, L.Y. Wu, T.J. Gentry, Y.F. Yin, J. Liebich, T.C. Hazen, J.Z. Zhou **GeoChip 3.0 as a high-throughput tool for analyzing microbial community composition, structure and functional activity**
ISME J., 4 (9) (2010), pp. 1167-1179
[CrossRefView Record in Scopus](#)

[Howard et al., 19](#)

P.C. Howard, F.A. Beland, C.E. Cerniglia **Reduction of the carcinogen 1-nitropyrene to 1-aminopyrene by rat intestinal bacteria**
Carcinogenesis, 4 (8) (1983), pp. 985-990
[CrossRefView Record in Scopus](#)

[Kim et al., 2015](#)

B.H. Kim, S.S. Lim, W.R. Daud, G.M. Gadd, I.S. Chang **The biocathode of microbial electrochemical systems and microbially-influenced corrosion**
Bioresour. Technol., 190 (2015), pp. 395-401
[ArticleDownload PDFView Record in Scopus](#)

[Kinouchi et al., 1](#)

T. Kinouchi, Y. Manabe, K. Wakisaka, Y. Ohnishi **Biotransformation of 1-nitropyrene in intestinal anaerobic bacteria**
Microbiol. Immunol., 26 (11) (1982), pp. 993-1005
[CrossRefView Record in Scopus](#)

[Koder et al., 200](#)

R.L. Koder, C.A. Haynes, M.E. Rodgers, D.W. Rodgers, A.F. Miller **Flavin thermodynamics explain the oxygen insensitivity of enteric nitroreductases**
Biochemistry, 41 (48) (2002), pp. 14197-14205
[CrossRefView Record in Scopus](#)

[Kong et al., 2014](#)

D. Kong, B. Liang, D.J. Lee, A. Wang, N. Ren **Effect of temperature switchover on the degradation of antibiotic chloramphenicol by biocathode bioelectrochemical system**
J. Environ. Sci., 26 (8) (2014), pp. 1689-1697
[ArticleDownload PDFView Record in Scopus](#)

[Kong et al., 2015](#)

D. Kong, B. Liang, H. Yun, H. Cheng, J. Ma, M. Cui, A. Wang, N. Ren **Cathodic degradation of antibiotics: characterization and pathway analysis**
Water Res., 72 (2015), pp. 281-292
[ArticleDownload PDFView Record in Scopus](#)

[Kong et al., 2015](#)

D.Y. Kong, B. Liang, H. Yun, J.C. Ma, Z.L. Li, A.J. Wang, N.Q. Ren **Electrochemical degradation of nitrofurans furazolidone by cathode: characterization, pathway and antibacterial activity analysis**

Chem. Eng. J., 262 (2015), pp. 1244-1251

[ArticleDownload](#) [PDFView](#) [Record in Scopus](#)

[Kracke et al., 2015](#)

F. Kracke, I. Vassilev, J.O. Kromer **Microbial electron transport and energy conservation-the foundation for optimizing bioelectrochemical systems**

Front. Microbiol., 6 (2015), p. 575, [10.3389/fmicb.2015.00575](#)

[Kumar et al., 2015](#)

R. Kumar, L. Singh, Z.A. Wahid, M.F.M. Din **Exoelectrogens in microbial fuel cells toward bioelectricity generation: a review**

Int. J. Energy Res., 39 (8) (2015), pp. 1048-1067

[CrossRefView](#) [Record in Scopus](#)

[Lettinga et al., 2001](#)

G. Lettinga, S. Rebac, G. Zeeman **Challenge of psychrophilic anaerobic wastewater treatment**

Trends Biotechnol., 19 (9) (2001), pp. 363-370

[ArticleDownload](#) [PDFView](#) [Record in Scopus](#)

[Liang et al., 2014](#)

B. Liang, H. Cheng, J.D. Van

Nostrand, J. Ma, H. Yu, D. Kong, W. Liu, N. Ren, L. Wu, A. Wang, D.J. Lee, J. Zhou **Microbial community structure and function of nitrobenzene reduction biocathode in response to carbon source switchover**

Water Res., 54 (2014), pp. 137-148

[ArticleDownload](#) [PDFView](#) [Record in Scopus](#)

[Liang et al., 2014](#)

B. Liang, H.Y. Cheng, D.Y. Kong, S.H. Gao, F. Sun, D. Cui, F.Y. Kong, A.J. Zhou, W.Z. Liu, N.Q. Ren, W.M. Wu, A.J. Wang, D.J. Lee **Accelerated reduction of chlorinated nitroaromatic antibiotic chloramphenicol by biocathode**

Environ. Sci. Technol., 47 (10) (2013), pp. 5353-5361

[CrossRefView](#) [Record in Scopus](#)

[Logan, 2009](#)

B.E. Logan **Exoelectrogenic bacteria that power microbial fuel cells**

Nat. Rev. Microbiol., 7 (5) (2009), pp. 375-381

[CrossRefView](#) [Record in Scopus](#)

[Lovley, 2012](#)

D.R. Lovley **Electromicrobiology**

Annu. Rev. Microbiol., 66 (2012), pp. 391-409

[CrossRefView Record in Scopus](#)

[Lu et al., 2011](#)

L. Lu, N.Q. Ren, X. Zhao, H.A. Wang, D. Wu, D.F. Xing **Hydrogen production, methanogen inhibition and microbial community structures in psychrophilic single-chamber microbial electrolysis cells**

Energy Environ. Sci., 4 (4) (2011), pp. 1329-1336

[CrossRefView Record in Scopus](#)

[McKeown et al.,](#)

R.M. McKeown, D. Hughes, G. Collins, T. Mahony, V. O'Flaherty **Low-temperature anaerobic digestion for wastewater treatment**

Curr. Opin. Biotechnol., 23 (3) (2012), pp. 444-451

[ArticleDownload PDFView Record in Scopus](#)

[Mu et al., 2009](#)

Y. Mu, K. Rabaey, R.A. Rozendal, Z. Yuan, J. Keller **Decolorization of azo dyes in bioelectrochemical systems**

Environ. Sci. Technol., 43 (13) (2009), pp. 5137-5143

[CrossRefView Record in Scopus](#)

[Okamoto et al., 2](#)

A. Okamoto, K. Hashimoto, K.H. Nealson **Flavin redox bifurcation as a mechanism for controlling the direction of electron flow during extracellular electron transfer**

Angew. Chem. Int. Ed., 53 (41) (2014), pp. 10988-10991

[CrossRefView Record in Scopus](#)

[Pham et al., 200](#)

C.A. Pham, S.J. Jung, N.T. Phung, J. Lee, I.S. Chang, B.H. Kim, H. Yi, J. Chun **A novel electrochemically active and Fe(III)-reducing bacterium phylogenetically related to *Aeromonas hydrophila*, isolated from a microbial fuel cell**

FEMS Microbiol. Lett., 223 (1) (2003), pp. 129-134

[ArticleDownload PDFCrossRefView Record in Scopus](#)

[Pokkuluri et al., 2](#)

P.R. Pokkuluri, Y.Y. Londer, N.E.C. Duke, M. Pessanha, X. Yang, V. Orshonsky, L.Orshonsky, J. E rickson, Y. Zagayanskiy, C.A. Salgueiro, M. Schiffer **Structure of a novel dodecaheme cytochrome *c* from *Geobacter sulfurreducens* reveals an extended 12 nm protein with interacting hemes**

J. Struct. Biol., 174 (1) (2011), pp. 223-233

[ArticleDownload PDFView Record in Scopus](#)

[Qu et al., 2015](#)

Y. Qu, Q. Ma, J. Deng, W. Shen, X. Zhang, Z. He, J.D. Van Nostrand, J. Zhou, J. Zhou **Responses of microbial communities to single-walled carbon nanotubes in phenol wastewater treatment systems**

Environ. Sci. Technol., 49 (7) (2015), pp. 4627-4635

[CrossRefView Record in Scopus](#)

[Radjenovic et al.](#)

J. Radjenovic, M.J. Farre, Y. Mu, W. Gernjak, J. Keller **Reductive electrochemical remediation of emerging and regulated disinfection byproducts**

Water Res., 46 (6) (2012), pp. 1705-1714

[ArticleDownload PDFView Record in Scopus](#)

[Rafii et al., 2003](#)

F. Rafii, R. Wynne, T.M. Heinze, D.D. Paine **Mechanism of metronidazole-resistance by isolates of nitroreductase-producing *Enterococcus gallinarum* and *Enterococcus casseliflavus* from the human intestinal tract**

FEMS Microbiol. Lett., 225 (2) (2003), pp. 195-200

[ArticleDownload PDFCrossRefView Record in Scopus](#)

[Richter et al., 20](#)

K. Richter, M. Schicklberger, J. Gescher **Dissimilatory reduction of extracellular electron acceptors in anaerobic respiration**

Appl. Environ. Microbiol., 78 (4) (2012), pp. 913-921

[CrossRefView Record in Scopus](#)

[Roldan et al., 20](#)

M. Roldan, E. Perez-Reinado, F. Castillo, C. Moreno-Vivian **Reduction of polynitroaromatic compounds: the bacterial nitroreductases**

FEMS Microbiol. Rev., 32 (3) (2008), pp. 474-500

[CrossRefView Record in Scopus](#)

[Ross et al., 2011](#)

D.E. Ross, J.M. Flynn, D.B. Baron, J.A. Gralnick, D.R. Bond **Towards electrosynthesis in *Shewanella*: energetics of reversing the Mtr pathway for reductive metabolism**

PLoS ONE, 6 (2) (2011), [10.1371/journal.pone.0016649](https://doi.org/10.1371/journal.pone.0016649)

[Rouf and Rigney](#)

M.A. Rouf, M.M. Rigney **Growth temperatures and temperature characteristics of *Aeromonas***

Appl. Microbiol., 22 (4) (1971), pp. 503-506

[View Record in Scopus](#)

[Schloss et al., 20](#)

P.D. Schloss, S.L. Westcott, T. Ryabin, J.R. Hall, M. Hartmann, E.B. Hollister, R.A. Lesniewski, B. B. Oakley, D.H. Parks, C.J. Robinson, J.W. Sahl, B. Stres, G.G. Thallinger, D.J. Van Horn, C.F. Weber **Introducing mothur: open-source, platform-independent, community-supported software for describing and comparing microbial communities**

Appl. Environ. Microbiol., 75 (23) (2009), pp. 7537-7541

[CrossRefView Record in Scopus](#)

W.V. Shaw, A.G. Leslie **Chloramphenicol acetyltransferase**

Annu. Rev. Biophys. Biophys. Chem., 20 (1991), pp. 363-386

[CrossRefView Record in Scopus](#)

J. Shen, Y. Zhang, X. Xu, C. Hua, X. Sun, J. Li, Y. Mu, L. Wang **Role of molecular structure on bioelectrochemical reduction of mononitrophenols from wastewater**

Water Res., 47 (15) (2013), pp. 5511-5519

[ArticleDownload PDFView Record in Scopus](#)

[Spain, 1995](#)

J.C. Spain **Biodegradation of nitroaromatic compounds**

Annu. Rev. Microbiol., 49 (1995), pp. 523-555

[CrossRefView Record in Scopus](#)

[Stewart and Massey, 1985](#)

R.C. Stewart, V. Massey **Potentiometric studies of native and flavin-substituted old yellow enzyme**

J. Biol. Chem., 260 (25) (1985), pp. 13639-13647

[View Record in Scopus](#)

[Strycharz et al., 2010](#)

S.M. Strycharz, S.M. Gannon, A.R. Boles, A.E. Franks, K.P. Nevin, D.R. Lovley **Reductive dechlorination of 2-chlorophenol by *Anaeromyxobacter dehalogenans* with an electrode serving as the electron donor**

Environ. Microbiol. Rep., 2 (2) (2010), pp. 289-294

[CrossRefView Record in Scopus](#)

[Strycharz et al., 2008](#)

S.M. Strycharz, T.L. Woodard, J.P. Johnson, K.P. Nevin, R.A. Sanford, F.E. Löffler, D.R. Lovley **Graphite electrode as a sole electron donor for reductive dechlorination of tetrachlorethene by *Geobacter lovleyi***

Appl. Environ. Microbiol., 74 (19) (2008), pp. 5943-5947

[CrossRefView Record in Scopus](#)

[Sydow et al., 2014](#)

A. Sydow, T. Krieg, F. Mayer, J. Schrader, D. Holtmann **Electroactive bacteria-molecular mechanisms and genetic tools**

Appl. Microbiol. Biotechnol., 98 (20) (2014), pp. 8481-8495

[CrossRefView Record in Scopus](#)

[Teixeira et al., 1997](#)

L.M. Teixeira, M.G. Carvalho, V.L. Merquior, A.G. Steigerwalt, D.J. Brenner, R.R. Facklam **Phenotypic and genotypic characterization of *Vagococcus fluvialis*, including strains isolated from human sources**

J. Clin. Microbiol., 35 (11) (1997), pp. 2778-2781

[View Record in Scopus](#)

[Tu et al., 2014](#)

Q. Tu, H. Yu, Z. He, Y. Deng, L. Wu, J.D. Van

Nostrand, A. Zhou, J. Voordeckers, Y.J. Lee, Y. Qin, C.L. Hemme, Z. Shi, K. Xue, T. Yuan, A. Wang, J. Zhou **GeoChip 4: a functional gene-array-based high-throughput environmental technology for microbial community analysis**

Mol. Ecol. Resour., 14 (5) (2014), pp. 914-928

[View Record in Scopus](#)

[Wang et al., 2011](#)

A.J. Wang, H.Y. Cheng, B. Liang, N.Q. Ren, D. Cui, N. Lin, B.H. Kim, K. Rabaey **Efficient reduction of nitrobenzene to aniline with a biocatalyzed cathode**

Environ. Sci. Technol., 45 (23) (2011), pp. 10186-10193

[CrossRefView Record in Scopus](#)

[Wang et al., 2015](#)

Z. Wang, D.H. Leary, A.P. Malanoski, R.W. Li, W.J. Hervey, B.J. Eddie, G.S. Tender, S.G. Yanosky, G.J. Vora, L.M. Tender, B. Lin, S.M. Strycharz-Glaven **A previously uncharacterized, nonphotosynthetic member of the chromatiaceae is the primary CO₂-fixing constituent in a self-regenerating biocathode**

Appl. Environ. Microbiol., 81 (2) (2015), pp. 699-712

[CrossRefView Record in Scopus](#)

[Yang et al., 2015](#)

Y. Yang, Y. Xiang, G. Sun, W.M. Wu, M. Xu **Electron acceptor-dependent respiratory and physiological stratifications in biofilms**

Environ. Sci. Technol., 49 (1) (2015), pp. 196-202

[CrossRefView Record in Scopus](#)

[Zhang et al., 2015a](#)

Q.Q. Zhang, G.G. Ying, C.G. Pan, Y.S. Liu, J.L. Zhao **Comprehensive evaluation of antibiotics emission and fate in the river basins of china: source analysis, multimedia modeling, and linkage to bacterial resistance**

Environ. Sci. Technol., 49 (11) (2015), pp. 6772-6782

[CrossRefView Record in Scopus](#)

[Zhang et al., 2015b](#)

X.Q. Zhang, H.J. Feng, Y.X. Liang, Z.Q. Zhao, Y.Y. Long, Y. Fang, M.Z. Wang, J. Yin, D.S. Shen **The relief of microtherm inhibition for p-fluoronitrobenzene mineralization using electrical stimulation at low temperatures**

Appl. Microbiol. Biotechnol., 99 (10) (2015), pp. 4485-4494

[CrossRefView Record in Scopus](#)

[Zhou et al., 2013](#)

A.F. Zhou, Z.L. He, Y.J. Qin, Z.M. Lu, Y. Deng, Q.C. Tu, C.L. Hemme, J.D. Van
Nostrand, L.Y.Wu, T.C. Hazen, A.P. Arkin, J.Z. Zhou **StressChip as a high-throughput tool for
assessing microbial community responses to environmental stresses**

Environ. Sci. Technol., 47 (17) (2013), pp. 9841-9849

[CrossRefView Record in Scopus](#)